FEW-SHOT LEARNING ON GRAPHS VIA SUPER-CLASSES BASED ON GRAPH SPECTRAL MEASURES

Anonymous authors
Paper under double-blind review

ABSTRACT

We propose to study the problem of few-shot graph classification in graph neural networks (GNNs) to recognize unseen classes, given limited labeled graph examples. Despite several interesting GNN variants being proposed recently for node and graph classification tasks, when faced with scarce labeled examples in the few-shot setting, these GNNs exhibit significant loss in classification performance. Here, we present an approach where a probability measure is assigned to each graph based on the spectrum of the graph's normalized Laplacian. This enables us to accordingly cluster the graph base-labels associated with each graph into super-classes, where the L^p Wasserstein distance serves as our underlying distance metric. Subsequently, a super-graph constructed based on the super-classes is then fed to our proposed GNN framework which exploits the latent inter-class relationships made explicit by the super-graph to achieve better class label separation among the graphs. We conduct exhaustive empirical evaluations of our proposed method and show that it outperforms both the adaptation of state-of-the-art graph classification methods to few-shot scenario and our naive baseline GNNs. Additionally, we also extend and study the behavior of our method to semi-supervised and active learning scenarios.

1 INTRODUCTION

The need to analyze graph structured data coupled with the ubiquitous nature of graphs (Borgwardt et al., 2005; Duvenaud et al., 2015; Backstrom & Leskovec, 2010; Chau et al., 2011), has given greater impetus to research interest in developing graph neural networks (GNNs) (Defferrard et al., 2016; Kipf & Welling, 2016; Hamilton et al., 2017; Velikovi et al., 2018) for learning tasks on such graphs. The overarching theme in GNNs is for each node's feature vector to be generated by passing, transforming, and recursively aggregating feature information from a given k-hop neighborhood surrounding the node. However, GNNs still fall short in the "few-shot" learning setting, where the classifier must generalize well after seeing abundant base-class samples (while training) and very few (or even zero) samples from a novel class (while testing). Given the scarcity and difficulty involved with generation of labeled graph samples, it becomes all the more important to solve the problem of graph classification in the few-shot setting.

Limitations and challenges: Recent work by Xu et. al. (Xu et al., 2019) indicated that most recently proposed GNNs were designed based on empirical intuition and heuristic approaches. They studied the representational power of these GNNs and identified that most neighborhood aggregation and graph-pooling schemes had diminished discriminative power. They rectified this problem with the introduction of a novel *injective* neighborhood aggregation scheme, making it as strong as the Weisfeiler-Lehman (WL) graph isomorphism test (Weisfeiler & Leman, 1968).

Nevertheless, the problem posed by extremely scarce novel-class samples in the few-shot setting remains to persist as a formidable challenge, as it requires more rounds of aggregation to affect larger neighborhoods and hence necessitate greater depth in the GNN. However, when it comes to GNNs, experimental studies have shown that an increase in the number of layers results in dramatic performance drops in GNNs (Wu et al., 2019; Li et al., 2018b).

Our work: Motivated by the aforementioned observations and challenges, our method does the following. We begin with a once-off preprocessing step. We assign a probability measure to each graph, which we refer to as a *graph spectral measure* (similar to (Gu et al., 2015)), based on the

spectrum of the graph's normalized Laplacian matrix representation. Given this metric space of graph spectral measures and the underlying distance as the L^p Wasserstein distance, we compute *Wasserstein barycenters* (Agueh & Carlier, 2011) for each set of graphs specific to a base class and term these barycenters as *prototype graphs*. With this set of prototype graphs for each base class label, we cluster the spectral measures associated with each prototype graph in Wasserstein space to create a super-class label.

Utilizing this super-class information, we then build a *graph of graphs* called a *super-graph*. The intuition behind this is to exploit the non-explicit and latent inter-class relationships between graphs via their spectral measures and use a GNN on this to also introduce a *relational inductive bias* (Battaglia et al., 2018), which in turn affords us an improved sample complexity and hence better combinatorial generalization given such few samples to begin with.

Given, the super-classes and the super-graph, we train our proposed GNN model for few-shot learning on graphs. Our GNN consists of a *graph isomorphism network* (GIN) Xu et al. (2019) as a *feature extractor* $F_\theta(.)$ to generate graph embeddings; on which subsequently acts our *classifier* $C(.)$ comprising of two components: (i) C^{sup}: a MLP layer to learn and predict the super class associated to a graph, and (ii) C^{GAT}: a *graph attention network* (GAT) to predict the actual class label of a graph. The overall loss function is a sum of the cross-entropy losses associated with C^{sup} and C^{GAT}. We follow *initialization based strategy* (Chen et al., 2019), with a training and fine-tuning phase, so that in the fine-tuning phase, the pre-trained parameters associated with $F_\theta(.)$ and C^{sup} are frozen, and the few novel labeled graph samples are used to update the weights and attention learned by C^{GAT}.

Our contributions: To the best of our knowledge, we are the first to introduce few shot learning on graphs for graph classification. Next, we propose an architecture that makes use of the graph's spectral measures to generate a set of super-classes and a super-graph to better model the latent relations between classes, followed by our GNN trained using an initialization method. Finally, we conduct extensive experiments to gain insight into our method. For example, in the 20-shot setting on the *TRIANGLES* dataset, our method shows a substantial improvement of nearly 7% and 20% over DL-based and unsupervised baselines, respectively.

2 Related Work

Few-shot learning in the computer vision community was first introduced by (Fei-Fei et al., 2006) with the intuition that learning the underlying properties of the base classes given abundant samples can help generalize better to unseen classes with few-labeled samples available. Various learning algorithms have been proposed in the *image domain*, among which a broad category of *initialization based methods* aim to learn transferable knowledge from training classes, so that the model can be adapted to unseen classes with limited labeled examples (Finn et al., 2017); (Rusu et al., 2018); (Nichol et al., 2018). Recently proposed and widely accepted *Initialization based methods* can broadly be classified into: (i) methods that learn good model parameters with limited labeled examples and a small number of gradient update steps (Finn et al., 2017) and (ii) methods that learn an optimizer (Ravi & Larochelle, 2017). We refer the interested reader to Chen et. al. (Chen et al., 2019) for more examples of few-shot learning methods in vision.

Graph neural networks (GNNs) were first introduced in (Gori et al., 2005); (Scarselli et al., 2009) as *recurrent message passing algorithms*. Subsequent work (Bruna et al., 2014); (Henaff et al., 2015) proposed to learn smooth spectral multipliers of the graph Laplacian, but incurred higher computational cost. This computational bottleneck was later resolved (Defferrard et al., 2016); (Kipf & Welling, 2016) by learning polynomials of the graph Laplacian. GNNs are a natural extension to Convolutional neural networks (CNNs) on non-Euclidean data. Recent work (Velikovi et al., 2018) introduced the concept of self-attention in GNNs, which allows each node to provide attention to the enclosing neighborhood resulting in improved learning. We refer the reader to (Bronstein et al., 2016) for detailed information on GNNs.

Despite all the success of GNNs, *few-shot classification* remains an under-addressed problem. Some recent attempts have focused on solving the few-shot learning on graph data where GNNs are either trained via co-training and self-training (Li et al., 2018a), or extended by stacking transposed graph

convolutional layers imputing a structural regularizer (Zhang et al., 2019) - however, both these works focus only on the node classification task.

To the best of our knowledge, there does not exist any work pertaining few-shot learning on graphs focusing on the graph classification task, thus providing the motivation for this work.

3 PRELIMINARIES

In this section, we introduce our notation and provide the necessary background for our few-shot learning setup on graphs. We begin by describing the various data sample types, followed by our learning procedure, in order to formally define few-shot learning on graphs. Finally, we define the *graph spectral distance* between a pair of graphs.

Data sample sets: Let $\mathcal{G}$ denote a set of undirected unweighted graphs and $\mathcal{Y}$ be the set of associated class labels. We consider two disjoint populations of labeled graphs consisting of i.i.d. graph samples, the set of *base class* labeled graphs $G_B = \{(g_i^{(B)}, y_i^{(B)})\}_{i=1}^{n}$ and the set of *novel class* labeled graphs $G_N = \{(g_i^{(N)}, y_i^{(N)})\}_{i=1}^{m}$, where $g_i^{(B)}, g_i^{(N)} \in \mathcal{G}$, $y_i^{(B)} \in \mathcal{Y}^{(B)}$, and $y_i^{(N)} \in \mathcal{Y}^{(N)}$. Here, the set of base and novel class labels are denoted by $\mathcal{Y}^{(B)} = \{1, \ldots, K\}$ and $\mathcal{Y}^{(N)} = \{K+1, \ldots, K'\}$, respectively, where $K' > K$. Both $\mathcal{Y}^{(B)}$ and $\mathcal{Y}^{(N)}$ are disjoint subsets of $\mathcal{Y}$, so, $\mathcal{Y}^{(B)} \cap \mathcal{Y}^{(N)} = \emptyset$.

Note that $m \ll n$, i.e., there are far fewer novel class labeled graphs compared to the base class labeled ones. Besides G_B and G_N, we consider a set of t unlabeled *unseen* graphs $G_U := \{g_1^{(U)}, \ldots, g_t^{(U)} \mid g_i^{(U)} \in \pi_1(G_N), i = 1 \ldots t\}$, for testing[1].

Learning procedure: Inspired by the *initialization based methods*, we similarly follow a two-stage approach of *training* followed by *fine-tuning*.

During training, we train a graph feature extractor $F_\theta(G_B)$ with network parameters θ followed by a classifier $C(G_B)$ on graphs from G_B, where the loss function is the standard cross-entropy loss $\mathcal{L}_c$. In order to better recognize and generalize well on samples from novel classes, in the fine-tuning phase, the pre-trained feature extractor $F_\theta(.)$ along with its trained parameters is fixed and the classifier $C(G_N)$ is trained on the novel class labeled graph samples from G_N, with the same loss $\mathcal{L}_c$.

Now, given the classification of data samples and the two-stage learning method, our problem of few-shot classification on graphs can be defined as follows.

Problem definition: Given n base-class labeled graphs from G_B during the training phase and m novel-class labeled graphs from G_N during the fine-tuning phase, where $m \ll n$, the objective of few-shot graph classification is to classify t unseen test graph samples from G_U. Moreover, if $m = qT$, where $T = K' - K$, i.e., each novel class label appears exactly q times in G_N, then this setting is referred to as the q-shot, T-way learning.

Graph spectral distance: Let us consider the graphs in $\mathcal{G}$. The normalized Laplacian of a graph $g \in \mathcal{G}$ is defined as $\Delta_g = I - D^{-1/2}AD^{1/2}$, where A and D are the adjacency and the degree matrices of graph g, respectively. The set of eigenvalues of Δ_g given by $\{\lambda_i\}_{i=1}^{|V|}$ is called the *spectrum* of Δ_g and is denoted by $\sigma(g)$. It is well known that the spectrum $\sigma(g)$ of a normalized Laplacian matrix is contained in interval $[0, 2]$. We assign a Dirac mass δ_{λ_i} concentrated on each $\lambda_i \in \sigma(g)$, thus associating a probability measure to $\sigma(g)$ supported on $[0, 2]$, called the *graph spectral measure* $\mu_{\sigma(g)}$. Furthermore, let $P([0, 2])$ be the set of probability measures on interval $[0, 2]$.

We now define the p-th Wasserstein distance between probability measures, which we later use to define the *spectral distance* between a pair of graphs.

Definition 1 *Let $p \in [1, \infty)$ and let $c : [0, 2] \times [0, 2] \to [0, +\infty]$ be the* cost function *between the probability measures $\mu, \nu \in P([0, 2])$. Then the p-th Wasserstein distance between measures μ and*

[1]We use the notation $\pi_1(p)$ and $\pi_2(p)$ to denote the left and right projection of an ordered pair p, respectively.

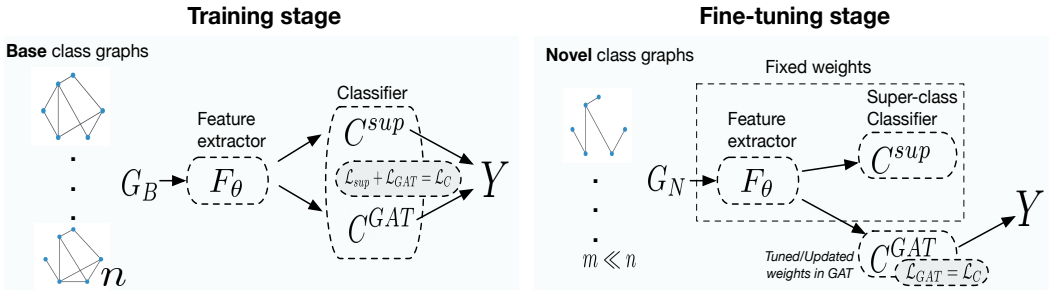

Figure 1: The training (left) and fine-tuning (right) stages of our GNN.

ν is given by

$$W_p(\mu, \nu) = \left(\inf_{\gamma} \int_{[0,2]\times[0,2]} c(x,y)^p d\gamma \mid \gamma \in \Pi(\mu, \nu) \right)^{\frac{1}{p}}$$

where $\Pi(\mu, \nu)$ is the set of transport plans*, i.e., the collection of all measures on $[0, 2] \times [0, 2]$ with marginals μ and ν.*

Given the general definition of the p-th Wasserstein distance between probability measures and the *graph spectral measure*, we can now define the spectral distance between a pair of graphs in $\mathcal{G}$.

Definition 2 *Given two graphs $g, g' \in \mathcal{G}$, the spectral distance between them is defined as*

$$W^p(g, g') := W_p\left(\mu_{\sigma(g)}, \mu_{\sigma(g')}\right)$$

In words, $W^p(g, g')$ is the optimal cost of moving mass from the graph spectral measure of graph g to that of graph g', where the cost of moving unit mass is proportional to the p-th power of the difference of real-eigenvalues in interval $[0, 2]$[2].

4 Our Method

We present our proposed approach here. First, given abundant base-class labels, we cluster them into *super-classes* by computing *prototype graphs* from each class, followed by clustering the prototype graphs based on their spectral properties. This clustering of prototype graphs induces a natural clustering on their corresponding class labels, resulting in super-classes (as outlined in Section 4.1). These super-classes are then used in the creation of a *super-graph* used further down by our GNN. Note that the creation of super-classes, followed by building a super-graph are a once-off process. The prototype graphs as well as the super-classes for the base classes can be stored in memory for further use.

Next, we explain our graph neural network's architecture which comprises of a *feature extractor* $F_\theta(.)$ and a *classifier* $C(.)$, described in Section 4.2. The classifier $C(.)$ is further subdivided into a classifier C^{sup} that predicts the superclass of a graph feature vector and a *graph attention network* (GAT) C^{GAT} to predict the graph's class label. Figure 1 illustrates the training and fine-tuning phases of our GNN.

4.1 Computing Super classes

In order to exploit inter-class relationships between base-class labels, we cluster them in the following manner. First, we partition the set G_B into *class-specific sets* $G^{(i)}$, for $i = 1 \ldots K$, where $G^{(i)}$ is the set of graphs with base-class label i. Thus, $G_B = \bigsqcup_{i=1}^{K} G^{(i)}$.

[2]In practice, extremely fast computation of $W^p(g, g')$ is achieved using a regularized optimal transport (OT) (Genevay et al., 2016), which makes use of the Sinkhorn algorithm.

Then, we compute class prototype graphs for each class-specific set. The class prototype graph for class i represented by p_i is given by

$$p_i = \underset{g_i \in \pi_1(G^{(i)})}{\operatorname{argmin}} \frac{1}{|G^{(i)}|} \sum_{j=1}^{|G^{(i)}|} W^p(g_i, g_j) \tag{1}$$

Essentially, the class prototype graph p_i for the i-th class is the graph with the least average spectral distance to the rest of the graphs in the same class. Given these K prototypes, we cluster them using Llyod's method (also known as k-means)[3].

Clustering prototype graphs: Given K unlabeled prototypes $p_1, \ldots, p_K \in \pi_1(G_B)$ and their associated spectral measures $\mu_{\sigma(p_1)}, \ldots, \mu_{\sigma(p_K)} \in P([0, 2])$. We rename the spectral measures as $s_1, \ldots, s_K$ to ease notation. Thus, our goal is to associate these spectral measures to *at most* k clusters, where $k \geq 1$ is a user defined parameter.

The k-means problem finds a k-partition $C = \{C_1, \ldots, C_k\}$ that minimizes the following objective that represents the overall distortion error of the clustering

$$\underset{C}{\operatorname{argmin}} \sum_{i=1}^{k} \sum_{s_i \in C_i} W_p(s_i, B(C_i)) \tag{2}$$

where s_i is a prototype graph in cluster C_i and $B(C_i)$ is the Wasserstein barycenter of the cluster C_i. The barycenter is computed as

$$B(C_i) = \underset{p \in P([0,2])}{\operatorname{argmin}} \sum_{j=1}^{|C_i|} W_p(p, s(i, j)) \tag{3}$$

where $s(i, j)$ denotes the j-th spectral measure in the i-th cluster C_i.

Llyod's algorithm: Given an initial set of Wasserstein barycenters $B^{(1)}(C_1), \ldots, B^{(1)}(C_k)$ of spectral measures at step $t = 1$, one uses the standard Lloyd's algorithm to find the solution by alternating between the *assignment* (Equation 4) and *update* (Equation 5) steps

$$C_i^{(t)} = \left\{ s_p : W_p(s_p, B^{(t)}(C_i)) \leq W_p(s_p, B^{(t)}(C_j)), \forall j, 1 \leq j \leq k, 1 \leq p \leq K \right\} \tag{4}$$

$$C_i^{(t+1)} = B(C_i^{(t)}) \tag{5}$$

Llyod's algorithm is known to converge to a local minimum (except in pathological cases, where it can oscillate between equivalent solutions). The final output is a grouping of the prototype graphs into k groups, which also induces a grouping of the corresponding base classes. We denote these class groups as super-classes and denote the set of super-classes as $\mathcal{Y}^{sup}$.

4.2 Our graph neural network

Feature extractor: To apply standard neural network architectures for downstream tasks we must embed the graphs in a finite dimensional vector space. We consider graph neural networks (GNNs) that employ the following *message-passing* architecture

$$H^{(j)} = M(A, H^{(j-1)}, \theta^{(j)})$$

where $H^{(j)} \in \mathbb{R}^{|V| \times d}$ are the node embeddings (i.e., messages) computed after j steps of the GNN and M is the message propagation function which depends on the adjacency matrix of the graph A, the trainable parameters of the jth layer $\theta^{(j)}$, and node embeddings $H^{(j-1)}$ generated from the previous step.

A recently proposed GNN called the *graph isomorphism network* (GIN) by Xu et al. (2019) was shown to be stronger than several popular GNN variants like GCN Kipf & Welling (2016) and GraphSAGE Hamilton et al. (2017). What makes GIN so powerful and sets it apart from the other GNN variants is its *injective* neighborhood aggregation scheme which allows it to be as powerful as

[3]We used the seeding method suggested in k-means++ (Arthur & Vassilvitskii, 2007)

the Weisfeiler-Lehman (WL) graph isomorphism test. Motivated by this finding, we chose GIN as our graph feature extractor. The message propagation scheme in GIN is given by

$$H^{(j)} = MLP((1+\epsilon)^j) \odot H^{(j-1)} + A^T H^{(j-1)}) \tag{6}$$

Here, ϵ is a layer-wise learnable scalar parameter and MLP represents a multi-layer perceptron with layer-wise non-linearities for more expressive representations. The full GIN model run R iterations of Equation 6 to generate final node embeddings which we represent by $H^{(R)}$. As features from earlier iterations can also be helpful in achieving higher discriminative power, embeddings $H^{(j)}$ from all R iterations are concatenated as

$$H_g = \Big\|_{j=1}^{R} H^{(j)} \ ,$$

Here, $H^{(j)} = \sum_{v \in V} H_v^{(j)}$, where $H_i^{(j)}$ represents the i-th node's embedding in the j-th iteration and $\|$ denotes a concatenation operator. H_g now contains the graph embedding of a graph g and is passed on to the classifier.

Classifier: Here, our objective is to improve the class separation produced by the graph embeddings of the feature extractor $F_\theta(.)$ and we do this by building a "graph of graph embeddings", called a *super-graph* g^{sup}, where each node is a graph feature vector. We then employ our classifier $C(.)$ on this super-graph to achieve better separation among the graph classes in the embedding space.

During training, we first build the super-graph g^{sup} on a batch of base-labeled graphs as a *collection* of k-NN graphs, where each constituent k-NN graph is built on the graphs belonging to the same super-class. g^{sup} is then passed through a multi-layered graph attention network C^{GAT} to learn the associated class probabilities. The features extracted from $F_\theta(.)$ are passed into the MLP network C^{sup} to learn the associated super-class labels. C^{sup} and C^{GAT} combine to form our classifier $C(.)$. The cross-entropy losses associated with C^{sup} and C^{GAT} are added to give the overall loss for $C(.)$. The intuition behind construction of g^{sup} to train C^{GAT} on was to further improve the existing cluster separation based on graph spectral measures by introducing a *relational inductive bias* (Battaglia et al., 2018) that is inherent to the GNN C^{GAT}.

Recall that we adopt an *initialization method* (described in 3). In our fine-tuning stage, novel class labeled graphs from G_N are input to the network. The pre-trained parameters learned by the feature extractor $F_\theta(.)$ are *fixed* and C^{sup} is used to infer the novel graph's super-class label, followed by creation of super-graph on the novel graph samples and finally updating the parameters in C^{GAT} through the loss.

5 Experimental Results

5.1 Baselines and Datasets

The standard graph classification datasets do not adequately satisfy the requirements for few-shot learning due to the dearth of unique class labels. Hence, we pick two new classification datasets, namely, *Letter-High* and *TRIANGLES*. The details and statistics for these datasets are given in Appendix A.1. As there do not exist any standard state-of-the-art methods for few-shot graph classification, we chose existing baselines for standard graph classification from both supervised and unsupervised methods.

For *supervised deep learning* baselines, we chose - GIN (Xu et al. (2019)), CapsGNN (Xinyi & Chen (2019)), and Diffpool (Lee et al. (2019)). We ran these methods with similar settings as ours, i.e., by partitioning the main model into *feature extraction* and *classifier* sub-models to compare them in a fair and informative manner. From the *unsupervised* category, we consider 4 powerful SOTA methods - AWE (Ivanov & Burnaev (2018)), Graph2Vec (Narayanan et al. (2017)), Weisfeiler-Lehman subtree Kernel (Shervashidze et al. (2011)), and Graphlet count kernel (Shervashidze et al. (2009)). Since we want to analyze the few-shot classification abilities of these models, we essentially want to find out how well these algorithms can achieve class separation. We use k-NN search on the output embeddings of these algorithms.

Further configuration and implementation details for the baselines can be found in Appendix A.2. We also emphasize the benefit of using a GNN as a classifier by showing the adaptation of our model to semi-supervised fine-tuning (in Appendix A.5) and active learning (in Appendix A.6) settings.

Table 1: Results for various few-shot scenarios on *Letter-High* and *TRIANGLES* datasets. The best results are highlighted in **bold** while the second best results are underlined.

Method	***Letter-High***			***TRIANGLES***		
	5-shot	10-shot	20-shot	5-shot	10-shot	20-shot
WL	65.27 ± 7.67	68.39 ± 4.69	72.69 ± 3.02	51.25 ± 4.02	53.26 ± 2.95	57.74 ± 2.88
Graphlet	33.76 ± 6.94	37.59 ± 4.60	41.11 ± 3.71	40.17 ± 3.18	43.76 ± 3.09	45.90 ± 2.65
AWE	40.60 ± 3.91	42.20 ± 2.87	43.12 ± 1.00	39.36 ± 3.85	42.58 ± 3.11	44.98 ± 1.54
Graph2Vec	66.12 ± 5.21	68.17 ± 4.26	70.28 ± 2.81	48.38 ± 3.85	50.16 ± 4.15	54.90 ± 3.01
Diffpool	58.69 ± 6.39	61.59 ± 5.21	64.67 ± 3.21	64.17 ± 5.87	67.12 ± 4.29	73.27 ± 3.29
CapsGNN	56.60 ± 7.86	60.67 ± 5.24	63.97 ± 3.69	65.40 ± 6.13	68.37 ± 3.67	73.06 ± 3.64
GIN	65.83 ± 7.17	69.16 ± 5.14	73.28 ± 2.17	63.80 ± 5.61	67.30 ± 4.35	72.55 ± 1.97
GIN-k-NN	63.52 ± 7.27	65.66 ± 8.69	67.45 ± 8.76	58.34 ± 3.91	61.55 ± 3.19	63.45 ± 2.76
OurMethod-GCN	68.69 ± 6.50	72.80 ± 4.12	75.17 ± 3.11	69.37 ± 4.92	73.11 ± 3.94	77.86 ± 2.84
OurMethod-GAT	$\mathbf{69.91 \pm 5.90}$	$\mathbf{73.28 \pm 3.46}$	$\mathbf{77.38 \pm 1.58}$	$\mathbf{71.40 \pm 4.34}$	$\mathbf{75.60 \pm 3.67}$	$\mathbf{80.04 \pm 2.20}$

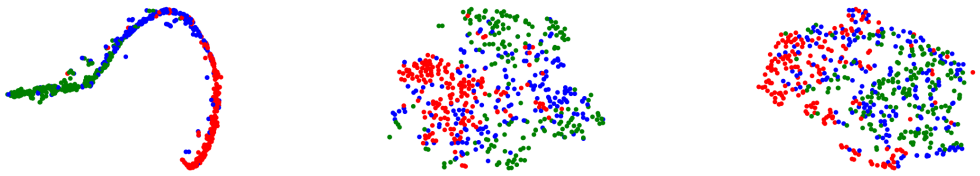

(a) Our Method-GAT (b) GIN (c) WL Kernel

Figure 2: Visualization: t-SNE plots of the computed embeddings of test graphs on 20-shot scenario from OurMethod-GAT (left), GIN (middle) and WL Kernel (right) on *TRIANGLES* dataset. The embeddings for both our model and GIN are taken from the final layers of the respective models.

5.2 Few-shot Results

We consider two variants of our model as *naive baselines*. In the first variant, we replace our GAT classifier with GCN Kipf & Welling (2016). We call this model *OurMethod-GCN*. This variant is used to justify the choice of GAT over GCN.

In the second variant, we replace the entire classifier with the k-NN algorithm over the features extracted from various layers of the *feature extractor*. We call this variant *GIN-k-NN* and this is introduced to emphasize the significance of building a super-graph and using a GAT on it as a classifier to exploit the relational inductive bias.

The results for all the datasets in various q-shot scenarios, where $q \in \{5, 10, 20\}$ are given in Table 1. We run each model 50 times and report averaged results. In every run, we select a different novel labeled subset G_N for fine-tuning the classifiers of the models. The evaluation for all models is done by randomly selecting a subset of 400 samples from the testing set G_U and averaging over 10 such random selections. The results clearly show that our proposed method and its GCN variant (i.e., *OurMethod-GCN*) outperform the baselines. GIN-k-NN shows significant degradation in results, thus strongly indicating that the improvements of our method can primarily be attributed to our GNN classifier. The improvements in results are higher on the *TRIANGLES* dataset in contrast to *Letter-High*, which can be attributed to the smaller size of the graphs in *Letter-High* making it difficult to distinguish based on graph spectra alone. GIN, WL, and Graph2Vec show much better results as compared to other baselines for all the q-shot scenarios, whereas AWE and Graphlet Kernel show significantly low results, unable to capture the properties of the graphs well. The DL baselines on the other hand show improvements on the *TRIANGLES* dataset, where the unsupervised methods fails to capture the local node properties. For the 20-shot scenario on *TRIANGLES*, our GAT variant shows an improvement of around 7% over DL baselines and more than 20% when compared to unsupervised methods. Furthermore, the t-SNE plots in Figure 3 show a substantial and interesting separation of class labels which strongly indicate that a good feature extractor in conjunction with a GNN perform well as a combination.

Table 2: Ablation Study: "No-SC" represents our classifier $C(.)$ without C^{sup} and "With-SC" represents $C(.)$ with both C^{sup} and C^{GAT} present.

Dataset	**10-shot**		**20-shot**	
	No-SC	With-SC	No-SC	With-SC
Letter-High	71.13 ± 3.64	73.61 ± 3.19	75.23 ± 2.48	77.42 ± 1.47
TRIANGLES	74.03 ± 3.89	76.49 ± 3.26	76.89 ± 2.63	80.14 ± 1.88

Table 3: Model analysis over number of super-classes in 20-shot scenario. Default value of parameter k is fixed at 2.

Dataset	**20-shot**				
	1	2	3	4	5
Letter-High	74.43 ± 2.61	76.61 ± 1.67	77.51 ± 1.49	76.31 ± 1.98	75.05 ± 2.29
TRIANGLES	76.43 ± 2.87	79.55 ± 1.91	80.51 ± 1.72	78.91 ± 2.09	78.25 ± 2.40

5.3 Ablation Study on Number of Super-Classes

Here, we study the behavior of our proposed network model without the super-class classifier C^{sup}. In Table 2 (10 and 20-shot setting), we observe a marked increase with the addition of our classifier which uses the super-class information and the super-graph based on spectral measures to guide C^{GAT} towards improving the class separation of the graphs during both the training and fine-tuning stages.

5.4 Sensitivity Analysis of Various Attributes

Our proposed method contains two crucial attributes. We analyze our model by varying: (i) the number of super-classes and (ii) the k-value in super-graph construction. The effect of varying these attributes on model accuracy are shown in Tables 3 and 4, respectively. As we increase the number of super-classes, we observe the accuracy improving steadily up to 3 super-classes and then dropping from there onwards. For super-classes less than 3, we observe that the k-NN graph does not respect the class boundaries that are already imposed by the graph spectral measures, thus connecting more arbitrary classes. On the other hand, increasing the number of super-classes past 3, makes each super-class cluster very sparse with few graph classes within, leading to an underflow of information between the graph classes.

The k-value or the number of neighbors of each node belonging to the same *connected component* in the super-graph (i.e., belonging to the same super-class) is another salient parameter upon which hinges the information flow (via message passing) between the graphs of the same super-class. We analyze our model with k values in the set $\{2, 4, 6, 8\}$ and a commonly used heuristic method, whereby each graph is connected to $\sqrt{b_s}$ nearest neighboring graphs based on the Euclidean similarity of their feature representations, where b_s is the number of samples in the mini-batch corresponding to super-classes s. We achieve best results with 2-NN graphs per super-class and increasing k beyond it leads to denser graphs with unnecessary connections between classes belonging to the same super-class.

Table 4: Model analysis over number of neighbors (k) in super-graph for 20-shot scenario. Default value for the number of super-classes is fixed at 3.

Dataset	**20-shot**				
	2	4	6	8	Heuristic
Letter-High	77.33 ± 1.71	76.61 ± 1.67	75.63 ± 2.49	74.66 ± 2.61	74.35 ± 2.48
TRIANGLES	80.77 ± 1.57	79.85 ± 1.59	79.45 ± 1.97	78.93 ± 2.04	79.42 ± 3.16

6 CONCLUSION

In this paper, we investigated the problem of few-shot learning on graphs for the graph classification task. We explicitly created a *super-graph* on the base-labeled graphs and then *grouped / clustered* their associated class labels into *super-classes*, based on the graph spectral measures attributed to each graph and the L^p-Wasserstein distances between them. We found that training our GNN on the super-graph along with the auxiliary super-classes resulted in a marked improvement over state-of-the-art GNNs. A promising future work is to propose new GNN models that break away from current neighborhood aggregation schemes to specifically overcome the obstacle posed by few-shot learning on graphs. Our source-code and dataset splits have been made public in an attempt to attract more attention to the context of few-shot learning on graphs.

REFERENCES

Martial Agueh and Guillaume Carlier. Barycenters in the wasserstein space. *SIAM J. Math. Analysis*, 43(2):904–924, 2011.

David Arthur and Sergei Vassilvitskii. K-means++: The advantages of careful seeding. In *Proceedings of the Eighteenth Annual ACM-SIAM Symposium on Discrete Algorithms*, SODA '07, pp. 1027–1035, 2007.

Lars Backstrom and Jure Leskovec. Supervised random walks: Predicting and recommending links in social networks. *CoRR*, abs/1011.4071, 2010. URL http://arxiv.org/abs/1011.4071.

Peter Battaglia, Jessica Blake Chandler Hamrick, Victor Bapst, Alvaro Sanchez, Vinicius Zambaldi, Mateusz Malinowski, Andrea Tacchetti, David Raposo, Adam Santoro, Ryan Faulkner, Caglar Gulcehre, Francis Song, Andy Ballard, Justin Gilmer, George E. Dahl, Ashish Vaswani, Kelsey Allen, Charles Nash, Victoria Jayne Langston, Chris Dyer, Nicolas Heess, Daan Wierstra, Pushmeet Kohli, Matt Botvinick, Oriol Vinyals, Yujia Li, and Razvan Pascanu. Relational inductive biases, deep learning, and graph networks. *arXiv*, 2018. URL https://arxiv.org/pdf/1806.01261.pdf.

Karsten M. Borgwardt, Cheng Soon Ong, Stefan Schönauer, S. V. N. Vishwanathan, Alex J. Smola, and Hans-Peter Kriegel. Protein function prediction via graph kernels. *Bioinformatics*, 21(1): 47–56, January 2005. ISSN 1367-4803. doi: 10.1093/bioinformatics/bti1007. URL http://dx.doi.org/10.1093/bioinformatics/bti1007.

Michael M. Bronstein, Joan Bruna, Yann LeCun, Arthur Szlam, and Pierre Vandergheynst. Geometric deep learning: going beyond euclidean data. *CoRR*, abs/1611.08097, 2016. URL http://arxiv.org/abs/1611.08097.

Joan Bruna, Wojciech Zaremba, Arthur Szlam, and Yann Lecun. Spectral networks and locally connected networks on graphs. In *International Conference on Learning Representations (ICLR2014), CBLS, April 2014*, 2014.

Duen Horng Chau, Carey Nachenberg, Jeffrey Wilhelm, Adam Wright, and Christos Faloutsos. Polonium: Tera-scale graph mining and inference for malware detection. In *SIAM INTERNATIONAL CONFERENCE ON DATA MINING (SDM)*, pp. 131–142, 2011.

Wei-Yu Chen, Yen-Cheng Liu, Zsolt Kira, Yu-Chiang Frank Wang, and Jia-Bin Huang. A closer look at few-shot classification. In *International Conference on Learning Representations*, 2019. URL https://openreview.net/forum?id=HkxLXnAcFQ.

Michaël Defferrard, Xavier Bresson, and Pierre Vandergheynst. Convolutional neural networks on graphs with fast localized spectral filtering. In D. D. Lee, M. Sugiyama, U. V. Luxburg, I. Guyon, and R. Garnett (eds.), *Advances in Neural Information Processing Systems 29*, pp. 3844–3852. Curran Associates, Inc., 2016.

David K Duvenaud, Dougal Maclaurin, Jorge Iparraguirre, Rafael Bombarell, Timothy Hirzel, Alan Aspuru-Guzik, and Ryan P Adams. Convolutional networks on graphs for learning molecular

fingerprints. In C. Cortes, N. D. Lawrence, D. D. Lee, M. Sugiyama, and R. Garnett (eds.), *Advances in Neural Information Processing Systems 28*, pp. 2224–2232. Curran Associates, Inc., 2015.

Li Fei-Fei, Rob Fergus, and Pietro Perona. One-shot learning of object categories. *IEEE Trans. Pattern Anal. Mach. Intell.*, 28(4):594–611, April 2006. ISSN 0162-8828. doi: 10.1109/TPAMI.2006.79. URL https://doi.org/10.1109/TPAMI.2006.79.

Chelsea Finn, Pieter Abbeel, and Sergey Levine. Model-agnostic meta-learning for fast adaptation of deep networks. *CoRR*, abs/1703.03400, 2017. URL http://arxiv.org/abs/1703.03400.

Aude Genevay, Marco Cuturi, Gabriel Peyré, and Francis Bach. Stochastic optimization for large-scale optimal transport. In *Advances in Neural Information Processing Systems 29*, pp. 3440–3448. 2016.

Marco Gori, Gabriele Monfardini, and Franco Scarselli. A new model for learning in graph domains. In *Proceedings. 2005 IEEE International Joint Conference on Neural Networks, 2005.*, volume 2, pp. 729–734. IEEE, 2005.

Jiao Gu, Bobo Hua, and Shiping Liu. Spectral distances on graphs. *Discrete Applied Mathematics*, 190-191:56 – 74, 2015.

William L. Hamilton, Rex Ying, and Jure Leskovec. Inductive representation learning on large graphs. *CoRR*, abs/1706.02216, 2017. URL http://arxiv.org/abs/1706.02216.

Mikael Henaff, Joan Bruna, and Yann LeCun. Deep convolutional networks on graph-structured data. *CoRR*, abs/1506.05163, 2015. URL http://arxiv.org/abs/1506.05163.

Sergey Ivanov and Evgeny Burnaev. Anonymous walk embeddings. In Jennifer Dy and Andreas Krause (eds.), *Proceedings of the 35th International Conference on Machine Learning*, volume 80 of *Proceedings of Machine Learning Research*, pp. 2186–2195, Stockholmsmssan, Stockholm Sweden, 10–15 Jul 2018. PMLR. URL http://proceedings.mlr.press/v80/ivanov18a.html.

Diederik P. Kingma and Jimmy Ba. Adam: A method for stochastic optimization, 2014. URL http://arxiv.org/abs/1412.6980. cite arxiv:1412.6980Comment: Published as a conference paper at the 3rd International Conference for Learning Representations, San Diego, 2015.

Thomas N. Kipf and Max Welling. Semi-supervised classification with graph convolutional networks. *CoRR*, abs/1609.02907, 2016. URL http://arxiv.org/abs/1609.02907.

Junhyun Lee, Inyeop Lee, and Jaewoo Kang. Self-attention graph pooling. In Kamalika Chaudhuri and Ruslan Salakhutdinov (eds.), *Proceedings of the 36th International Conference on Machine Learning*, volume 97 of *Proceedings of Machine Learning Research*, pp. 3734–3743, Long Beach, California, USA, 09–15 Jun 2019. PMLR. URL http://proceedings.mlr.press/v97/lee19c.html.

Qimai Li, Zhichao Han, and Xiao-Ming Wu. Deeper insights into graph convolutional networks for semi-supervised learning. *CoRR*, abs/1801.07606, 2018a. URL http://arxiv.org/abs/1801.07606.

Qimai Li, Zhichao Han, and Xiao-Ming Wu. Deeper insights into graph convolutional networks for semi-supervised learning. In *AAAI*, 2018b.

Annamalai Narayanan, Mahinthan Chandramohan, Rajasekar Venkatesan, Lihui Chen, Yang Liu, and Shantanu Jaiswal. graph2vec: Learning distributed representations of graphs. *CoRR*, abs/1707.05005, 2017. URL http://arxiv.org/abs/1707.05005.

Alex Nichol, Joshua Achiam, and John Schulman. On first-order meta-learning algorithms. *CoRR*, abs/1803.02999, 2018. URL http://arxiv.org/abs/1803.02999.

Sachin Ravi and Hugo Larochelle. Optimization as a model for few-shot learning. In *5th International Conference on Learning Representations, ICLR 2017, Toulon, France, April 24-26, 2017, Conference Track Proceedings*. OpenReview.net, 2017. URL https://openreview.net/forum?id=rJY0-Kcll.

Andrei A. Rusu, Dushyant Rao, Jakub Sygnowski, Oriol Vinyals, Razvan Pascanu, Simon Osindero, and Raia Hadsell. Meta-learning with latent embedding optimization. *CoRR*, abs/1807.05960, 2018. URL http://arxiv.org/abs/1807.05960.

Franco Scarselli, Marco Gori, Ah Chung Tsoi, Markus Hagenbuchner, and Gabriele Monfardini. The graph neural network model. *Trans. Neur. Netw.*, 20(1):61–80, January 2009. ISSN 1045-9227. doi: 10.1109/TNN.2008.2005605. URL http://dx.doi.org/10.1109/TNN.2008.2005605.

N. Shervashidze, SVN. Vishwanathan, TH. Petri, K. Mehlhorn, and KM. Borgwardt. Efficient graphlet kernels for large graph comparison. In *JMLR Workshop and Conference Proceedings Volume 5: AISTATS 2009*, pp. 488–495, Cambridge, MA, USA, April 2009. Max-Planck-Gesellschaft, MIT Press.

Nino Shervashidze, Pascal Schweitzer, Erik Jan van Leeuwen, Kurt Mehlhorn, and Karsten M. Borgwardt. Weisfeiler-lehman graph kernels. *J. Mach. Learn. Res.*, 12:2539–2561, November 2011. ISSN 1532-4435. URL http://dl.acm.org/citation.cfm?id=1953048.2078187.

Petar Velikovi, Guillem Cucurull, Arantxa Casanova, Adriana Romero, Pietro Li, and Yoshua Bengio. Graph attention networks. In *International Conference on Learning Representations*, 2018. URL https://openreview.net/forum?id=rJXMpikCZ.

B. Yu. Weisfeiler and A. A. Leman. Reduction of a graph to a canonical form and an algebra arising during this reduction. 1968.

Zonghan Wu, Shirui Pan, Fengwen Chen, Guodong Long, Chengqi Zhang, and Philip S. Yu. A comprehensive survey on graph neural networks. *CoRR*, abs/1901.00596, 2019.

Zhang Xinyi and Lihui Chen. Capsule graph neural network. In *International Conference on Learning Representations*, 2019. URL https://openreview.net/forum?id=Byl8BnRcYm.

Keyulu Xu, Weihua Hu, Jure Leskovec, and Stefanie Jegelka. How powerful are graph neural networks? In *International Conference on Learning Representations*, 2019. URL https://openreview.net/forum?id=ryGs6iA5Km.

Shengzhong Zhang, Ziang Zhou, Zengfeng Huang, and Zhongyu Wei. Few-shot classification on graphs with structural regularized GCNs, 2019. URL https://openreview.net/forum?id=r1znKiAcY7.

A APPENDIX

A.1 DATASET DETAILS

As there are no standard benchmarks available for few-shot graph classification, we picked 2 new datasets *Letter-High* and *TRIANGLES*. These datasets can be downloaded here [4]. The dataset statistics are provided in Table 5, while the split statistics are provided in Table 6

Table 5: Dataset Statistics

Dataset Name	**# Classes**	**# Graphs**	**Avg # Nodes**	**Avg # Edges**
Letter-High	15	2250	4.67	4.50
TRIANGLES	10	45000	20.85	35.50

Table 6: Dataset Statistics

Dataset Name	**# Train Classes**	**# Test Classes**	**# Training Graphs**	**# Validation Graphs**	**# Test Graphs**
Letter-High	11	4	1330	320	600
TRIANGLES	7	3	1126	271	603

The validation graphs are used to assess model performance on training classes itself to check overfitting as well as for grid-search over hyperparameters. The actual train-testing class splits used for this paper are provided with the code. Since the TRIANGLES dataset has a large number of samples, this makes it infeasible to run many baselines including DL and non-DL methods. Hence, we sample 200 graphs from each class, making the total sample size 2000.

A.2 BASELINE DETAILS

This section details the implementation of the baseline methods. Since, DL-based methods - GIN, CapsGNN and DIFFPOOL have not been previously run on these datasets, we select the crucial hyper-parameters - such as number of layers heuristically based on the results of standard graph classification datasets on the best performing variants of these models. For these three methods we take the novel layers proposed in the corresponding papers as their feature extractors, while downstream MLP layers are chosen as the classifier. The training and evaluation strategies are similar to our model, i.e., the models are first trained in an end-to-end fashion on the training dataset G_B until convergence with learning rate decay on loss plateau and then the classifier layers are fine-tuned over G_N, keeping the parameters of the feature extractor layers fixed.

For the unsupervised models - WL subtree kernel, Graphlet Count kernel, AWE and Graph2Vec, the evaluation is done using k-NN search to assess the clustering quality of these models in our few-shot scenario. We refrain from using high-level classifier models such as SVM or MLPs, since training these classifiers on few-shot regime will not properly assess the abilities of these models to cluster together graphs of similar class labels. We empirically found that using high level classifiers resulted in higher deviations and lower mean accuracies. We choose the hyper-parameters for these models using grid-search, since they are significantly faster and each one of these models have few highly sensitive parameters which affect the model significantly. For these models, we perform a grid search for selection of k in the k-NN algorithm from the set $\{1, 2, 3, 4, 5\}$ for the 5-shot scenario, of which $k = 1$ was found to perform the best. For higher shot scenario, the search was performed over the set $\{1, 2, 3, 4, 5, 6, 7, 8, 9, 10\}$, where we again found $k = 1$ to be the best. The validation set is used to check overfitting and hyper-parameter selection on the baseline methods.

[4] https://ls11-www.cs.tu-dortmund.de/staff/morris/graphkerneldatasets

A.3 OUR MODEL DETAILS

This section provides the implementation details of our proposed model. Since, our feature extractor model is GIN, we maintain similar parameter settings as recommended by their paper. As mentioned in section 4.2, using embeddings from all iterations of the message passing network helps achieve better discriminative power and improved gradient flow, therefore we employ the same strategy in our feature extractor. The number of super-classes are selected from the set $\{1, 2, 3, 4, 5\}$ using grid-search. The k-value for construction of super-graph was selected from the set $\{2, 4, 6, 8\}$. The feature extractor model uses *batch-normalization* between subsequent message passing layers. We use dropout of 0.5 in the C^{sup} layers. The C^{GAT} layers undergo normalization of inputs between subsequent layers along with a dropout of 0.5, however, the normalization mechanism in classifier layers is different from batch-norm. We normalize each feature embedding to have Euclidean norm with value 1. Essentially,

$$\mathbf{x}_{input}^{j+1} = \frac{\mathbf{x}_{out}^{j}}{||\mathbf{x}_{out}^{j}||_2} \tag{7}$$

where $\mathbf{x}_{input}^{j+1}$ is the input of $j+1^{th}$ layer of classifier, $\mathbf{x}_{out}^{j}$ is the output of the jth layer. The inputs of the first layer of C^{GAT} also undergo the same transformation over the outputs of the feature extractor model. We train our models with Adam (Kingma & Ba (2014)) with an initial learning rate of 10^{-3} for 50 epochs. Each epoch has 10 iterations, where we randomly select a mini-batch from the training data G_B. The fine-tuning stage consists of 20 epochs with 10 iterations per epoch. We use a two-layer MLP over the final attention layer of C^{GAT} for classification. The attention layers use multi-head attention with 2 heads and leaky ReLU slope of 0.1 . The embeddings from both the attention heads are concatenated. For 20-shot, we set k to 2 and batch size to 128 on the *Letter-High* dataset, while k is set to 2 and batch size 64 on *TRIANGLES* dataset. The number of super-classes is fixed at 3 for both the datasets. We used *Python Optimal Transport* (POT) library [5] for implementation of the p-th Wasserstein distance.

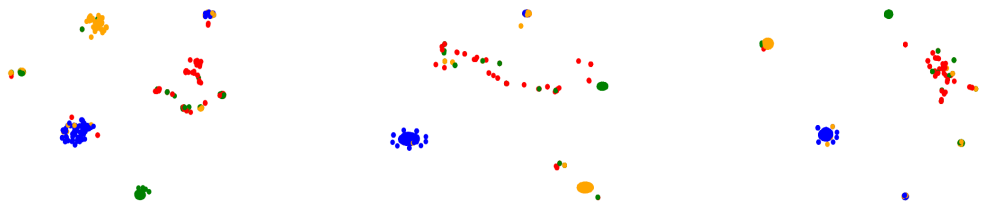

(a) Our Model (b) GIN (c) WL Kernel

Figure 3: Visualization: t-SNE plots of the computed embeddings of test graphs on 20-shot scenario from OurMethod-GAT (left), GIN (middle) and WL Kernel (right) on *Letter-High* dataset.

A.4 SILHOUETTE SCORES

To assess the clustering abilities of the models we analyze the *silhouette scores* of the test embeddings produced by the GAT variant of our method, GIN and WL Kernel. Silhouette coefficient essentially measures the ratio of intra-class versus inter-class distance. The Silhouette Coefficient is calculated using the mean intra-cluster distance (a) and the mean nearest-cluster distance (b) for each sample. The Silhouette Coefficient for a sample is given by $\frac{(b-a)}{max(a,b)}$,where b is the distance between a sample and the nearest cluster that the sample is not a part of. The results for mean silhouette coefficient over the test samples averaged over multiple runs are shown in Table 7. We normalize the embeddings before calculating the silhouette coefficient. We can clearly see that our model creates better clusters with low intra-cluster distance as well as high inter-cluster distance. Note that coefficient for WL remains the same for all scenarios since it computes fixed embeddings attributed to absence of any DL component.

[5] https://pot.readthedocs.io/en/stable/all.html

Table 7: Silhouette coefficients of the test classes for the three dominant models - GAT variant of Our Method, GIN and WL. The best scores are highlighted in bold.

Method	**Letter-High**		***TRIANGLES***	
	10-shot	20-shot	10-shot	20-shot
GIN	0.2157	0.2316	0.0373	0.1256
WL Kernel	0.2490	0.2490	0.0186	0.0186
OurMethod-GAT	**0.3494**	**0.3787**	**0.3824**	**0.4508**

Table 8: Semi-supervised fine-tuning results for various p values on 10-shot and 20-shot scenarios, where "No Semi-Sup" represents the fine-tuning stage without additional labeled samples.

Dataset	**10-shot**			**20-shot**		
	No Semi-Sup	25	50	No Semi-Sup	25	50
Letter-High	73.21 $\pm$ 3.19	74.18 $\pm$ 2.58	74.65 $\pm$ 2.16	76.95 $\pm$ 1.79	77.79 $\pm$ 1.52	78.31 $\pm$ 1.11
TRIANGLES	75.83 $\pm$ 2.97	76.36 $\pm$ 2.59	77.8 $\pm$ 2.04	80.09 $\pm$ 1.78	81.29 $\pm$ 1.98	81.87 $\pm$ 1.45

A.5 Semi-Supervised Fine-tuning

In many real-world learning scenarios, it is quite common to find abundant unlabelled data. Since our model uses a GNN classifier, this makes it possible to use unlabelled data while learning through message passing, where the fine tuning stage of our method is performed in semi-supervised settings.

Essentially, while fine tuning the model, i.e., only training the classifier C^{GAT} on G_N, we additionally use p more graphs along with G_N, whose labels are unknown. The learning objective for fine tuning stage doesn't change since the gradients are back-propagated from the labeled samples only. In this setting, each node in the attention classifier can aggregate information from unlabelled samples as well, thus allowing improved learning of the graphs features in C^{GAT}. We show the results for p values 25 and 50. The results are shown in Table 8. We observe an increase in the accuracy with increase in number of unlabeled samples during fine-tuning phase.

A.6 Adaptation to Active-Learing

In this section, we show the adaptation of our model to highly practical *active learning* scenario. In many real world applications, we might start with few samples per classes, however as the number of samples to classify from these classes increase over time, some of these samples can be used by the model to adaptively learn and improve with very less human intervention, since the number of number of samples to be queried for theirs label can always be controlled.

To perform active-learning, we first select a random subset of size 100 which we term as G_{random}, then fine tune the model on G_N and further evaluate the model on G_{random}. Thereafter, l *relatively important* samples are chosen from G_{random} and added to G_N for another step of fine-tuning. There can be multiple strategies for defining relative importance of a sample. For our purpose, we define a sample's relative importance via its predicted class probability distribution. We sort these samples in increasing order of the difference between their highest and second highest predicted class probabilities and choose the first l samples from this sorted ranking. We call this importance relative, since each sample is evaluated with respect to the set G_N and thus, there is transductive flow of information among the samples, hence defining the relative embeddings in the space. Intuitively speaking, we have chosen the samples lying closer to separation boundary with respect to G_N. The

Table 9: Active Learning Results. The value below each shot represents the number samples l, added to G_N for second fine-tuning step, where "No AL" represents the model evaluation without additional labeled samples.

Dataset	**10-shot**			**20-shot**		
	No AL	15	25	No AL	15	25
Letter-High	73.34 $\pm$ 3.37	75.03 $\pm$ 3.24	76.89 $\pm$ 2.16	77.06 $\pm$ 1.73	78.44 $\pm$ 1.52	79.28 $\pm$ 1.36
TRIANGLES	76.02 $\pm$ 2.54	78.44 $\pm$ 1.84	79.91 $\pm$ 1.28	80.27 $\pm$ 1.84	81.74 $\pm$ 2.03	82.58 $\pm$ 1.57

results for various values of l are shown in Table 9. The evaluation is done as mentioned earlier on the unseen set G_U. We observe significant improvement in the 10-shot scenario for both the datasets. This shows our model is capable of selecting important samples with respect to the few existing samples and learn actively.